Near-threshold infrared photodetachment of Al^-: A determination of the electron affinity of aluminum and the range of validity of the Wigner law

D. Calabrese, A. M. Covington, and J. S. Thompson
Department of Physics, University of Nevada, Reno, Reno, Nevada 89557-0058

R. W. Marawar* and John W. Farley
Department of Physics, University of Nevada, Las Vegas, 4505 South Maryland Parkway, Las Vegas, Nevada 89154-4002
(Received 3 January 1996; revised manuscript received 13 June 1996)

The relative photodetachment cross section of Al^- has been measured in the wavelength range 2420–2820 nm (0.440–0.512 eV), using a coaxial ion-laser beams apparatus, in which a 2.98-keV Al^- beam is merged with a beam from an F-center laser. The cross-section data near the $^3P_{0,1,2} \rightarrow {}^2P_{1/2,3/2}$ photodetachment threshold have been fitted to the Wigner threshold law and to the zero-core-contribution theory of photodetachment. The electron affinity of aluminum was determined to be 0.44094(+0.00066/−0.00048) eV, after correcting the experimental threshold for unresolved fine structure in the ground states of Al^- and Al. The new measurement is in agreement with the best previous measurement (0.441±0.010 eV) and is 20 times more precise. The Wigner law agrees with experiment within a few percent for photon energies within 3% of threshold. A proposed leading correction to the Wigner law is discussed. [S1050-2947(96)12009-6]

PACS number(s): 32.10.Hq, 32.80.Gc

I. INTRODUCTION

Negative ions are important in a variety of applications [1]: in the upper atmosphere, the formation of negative ions is the key factor limiting the density of free electrons, thereby affecting the conductivity of the upper atmosphere. Negative ions are important in the atmosphere of the Sun, and presumably of other stars as well. An important contribution to the opacity of the solar atmosphere is the photodetachment of H^-, as first discovered by Wildt [2]. In laboratory plasmas, negative ions affect voltage breakdown and current buildup. In addition, negative ions are important in tandem accelerators, in the electron-capture detector, and in other applications. In fundamental physics, negative ions are good systems for studying electron correlation, which typically plays a larger role in understanding negative ions than it does in positive ions or neutral atoms.

The importance of electron correlation is illustrated by the following example: in calculating the ionization potential of a neutral atom, one can neglect both the electron correlation and the core relaxation. The two effects are comparable in magnitude and opposite in sign. This fortuitous cancellation allows the calculation of relatively accurate results (e.g., 0.1 eV) using simple approaches. In contrast, in calculating the electron affinity of a negative ion, the electron correlation energy and the core relaxation energy have the same sign: they reinforce rather than cancel. Thus, it is necessary to know both in order to obtain an accurate result [3].

The photodetachment of a negative ion is fundamentally different from ionizing a neutral atom. In the former case, the departing electron leaves behind a neutral atom, while in the latter case, the departing electron leaves behind a positively charged core. Thus, the long-range Coulomb interaction between electron and core, which is present in the ionization of neutral atoms, is absent in the detachment of negative ions. Negative ions are thus good systems for studying high-order effects, which are presumably also present in neutral atoms, but are masked by the stronger Coulomb potential.

The behavior of photodetachment cross sections near threshold is widely believed to be governed by the Wigner law, but there have been relatively few direct experimental tests [4] of the Wigner law, particularly of the accuracy and range of validity of the Wigner law.

In this paper, we discuss the previous work on the subject, describe our experimental apparatus and technique, and present our experimental results. After our analysis and discussion, we conclude with some remarks for future work.

A. Previous theoretical work

Over four decades ago, Wigner [5] proposed a theory of the behavior of the cross section near threshold. Later, O'Malley [6] discovered a correction term that is proportional to the polarizability of the neutral species. Engelking [7] discovered that if the neutral species is a molecule with nonzero angular momentum about the axis of symmetry (e.g., a diatomic molecule in a non-Σ electronic state), the Wigner law requires modification. Engelking's discovery was subsequently applied to the photodetachment of OH^- by Herrick and Engelking [8]. Farley [9] studied the range of validity of the Wigner law theoretically, and proposed estimates for the size of the leading correction to the Wigner law. Very recently, Liu and Starace [10] calculated the photodetachment cross section for Al^-.

B. Previous experimental work

There have been very few experimental studies that test the Wigner law as applied to photodetachment. The first reliable verification of the Wigner law for photodetachment

*Present address: National Instruments, 6504 Bridge Point Parkway, Austin, TX 78730-5039.

was by Lineberger and Woodward [11], who studied S^-, corresponding to photodetachment from a *p* orbital. Other near-threshold studies of photodetachment from a *p* orbital include that by Hotop, Patterson, and Lineberger [12], who studied Se^- near threshold in the visible, and Feldmann [13], who observed photodetachment of C^-. Near-threshold studies of photodetachment from an *s* orbital include a study by Hotop and Lineberger [14] of Au^- in the visible, and a study by Lineberger and co-workers of H^- in the infrared [15].

Laser photodetachment threshold (LPT) studies of negative ions can produce very precise values of atomic electron affinities. LPT studies involve measurement of the photodetachment cross section as a function of photon energy. This technique has been used to make the most precise measurements of electron affinities to date: the electron affinities of atomic oxygen and sulfur have been measured [16] to a fraction of 1 part per 10^6. The most precise previous measurement of the electron affinity of aluminum was the laser photoelectron spectrometry (LPES) study of Feigerle *et al.* [17] who reported an electron affinity (EA) of 0.442 ± 0.010 eV. This value was adjusted slightly when the electron affinity of O^-, the calibrating ion for LPES studies, was remeasured in a precision measurement by Neumark *et al.* [18]. This resulted in a lowering (by 1 meV) of all previously measured EA values that were determined relative to O^-. Consequently, Hotop and Lineberger [16] recommended a value for Al^- of 0.441 ± 0.010 eV. The change in the EA of -1 ± 10 meV is not significant. In the study by Feigerle *et al.*, as in most LPES investigations, the overall precision of the measurement was limited by the 10-meV energy resolution of the electron spectrometer. In this paper, we present the results of an LPT study on Al^-, in order to determine a more precise value of the electron affinity of atomic aluminum. In addition, we compare the range of validity of the Wigner law for photodetachment of Al^- with the results of a recent calculation [9].

Theoretically, the photodetachment cross section can be expressed as a product of the square of the electric dipole transition element for exciting an electron from the bound state of the negative ion to a continuum state of the neutral atom and a departing electron, and the density of continuum states. Wigner [5] showed that near threshold the leading term describing the shape of the cross section curve is of the form

$$\sigma \sim E^{\ell+1/2} = (\hbar\omega - E_0)^{\ell+1/2}, \tag{1}$$

where E is the kinetic energy of the free electron in the center-of-mass frame of the negative ion, $\hbar\omega$ is the incident photon energy, E_0 is the threshold energy or electron affinity, and ℓ is the orbital angular momentum of the free electron. The threshold law is a consequence of the behavior of the interaction potential at long range, where the dominant term is the centrifugal barrier term. The threshold energy can be extracted from the photodetachment cross section data by fitting the near-threshold data to the Wigner threshold law. The electron affinity can be derived from the threshold energy, after making appropriate corrections for unresolved fine structure in the ion and neutral atom [16].

In the present experiment, a 2.98-keV beam of Al^- was merged coaxially with an infrared laser beam from an

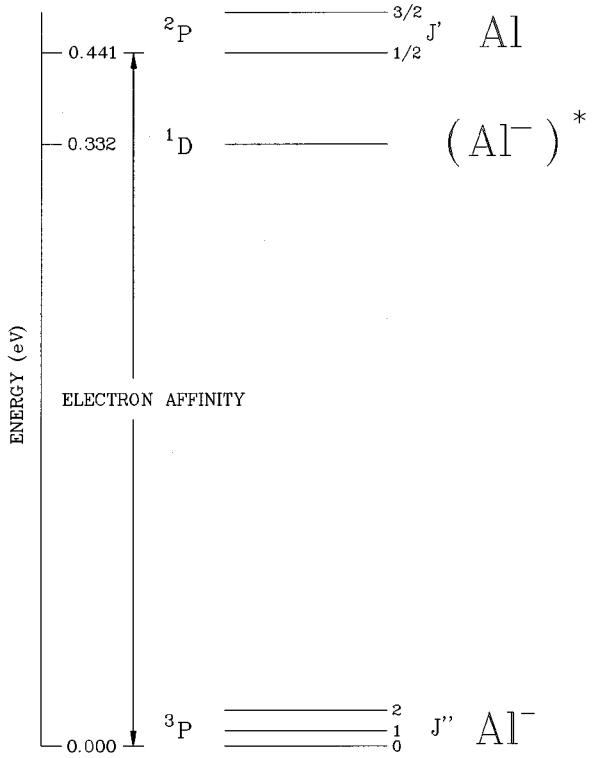

FIG. 1. Energy-level diagram for the photodetachment of Al^-. The fine-structure splittings for the ground states of the negative ion and neutral atom are shown. The splittings are exaggerated and are not to scale. The extrapolated ^3P energy differences for the $0\rightarrow1$ and $0\rightarrow2$ J'' splittings are $0.0032\pm0.000\,37$ eV (26 ± 3 cm^{-1}) and $0.0094\pm0.000\,87$ eV (76 ± 7 cm^{-1}), respectively. The ^2P energy difference for the J' splitting is 0.0139 eV (112 ± 0.01 cm^{-1}). The electron affinity of Al is defined as the transition from the $^3P_0$ state of Al^- to the $^2P_{1/2}$ of Al. Also shown is the metastable excited $^1D_2$ state of Al^-. Data for the diagram were obtained from Hotop and Lineberger (Ref. [16]), Feigerle *et al.* (Ref. [17]), and Moore (Ref. [28]).

F-center laser. The intensity of fast neutral atoms produced in the detachment process was measured as a function of photon energy to give the relative photodetachment cross section of Al^- in the wavelength range 2420–2820 nm (0.51–0.44 eV). The near-threshold cross section data were fitted to the Wigner threshold law [5] and the zero-core-contribution (ZCC) theory of photodetachment [19] to extract the electron affinity of aluminum. This measurement provides both an improved value of the electron affinity of Al, and the shape of the photodetachment cross section as a function of photon energy.

Photodetachment occurs between a number of fine-structure levels in the ion and the neutral atom. Figure 1 illustrates the relevant atomic energy levels. The electron affinity is defined as the energy needed to excite the electron from the lowest ($^3P_0$) state of Al^- to the lowest ($^2P_{1/2}$) state of Al. Engelking and Lineberger [20] demonstrated the photodetachment selection rules for transitions between the fine-structure components of the *LS*-coupled states of a negative ion and a neutral atom. In addition, they also showed that the relative intensities of these transitions depend upon a product of statistical and geometrical factors, and can be expressed as

TABLE I. Calculated relative intensities of the fine-structure components of the photodetachment transition from the ^3P state of Al^- to the ^2P state of Al. The table shows the relative intensity of $J''\rightarrow J'$ transitions, where $J''(J')$ represents an ionic (neutral) fine-structure level.

J'/J''	$J''=0$	$J''=1$	$J''=2$
$J'=1/2$	4/54	9/54	5/54
$J'=3/2$	2/54	9/54	25/54

$$I(J',J'')\sim\sum_{j=l-1/2}^{j=l+1/2}(2J'+1)(2J''+1)(2j+1)\times\begin{Bmatrix} S'' & L'' & J'' \\ \frac{1}{2} & l & j \\ S' & L' & J' \end{Bmatrix}^2, \quad (2)$$

where l and j are the orbital and total angular momentum quantum numbers of the detached electron, and S'',L'',J'' and S',L',J' are the spin, orbital, and total angular momentum quantum numbers for the negative ion and atom, respectively. In the present study, all $J''\rightarrow J'$ transitions are allowed. Their relative intensities have been calculated and are presented in Table I. In principle, it is possible to resolve individual fine-structure ($J''\rightarrow J'$) thresholds in an experiment with sufficient energy resolution and strong enough signals. In the present experiment, the fine structure is unresolved. Finally, the Al^- ion also has a metastable $^1D_2$ state that can contribute to the photodetachment signal, because the laser frequency is well above the photodetachment threshold of the metastable state.

II. EXPERIMENT

The experimental apparatus consists of two major components: a negative-ion source and the coaxial ion-laser beams interaction apparatus, shown in Fig. 2. The negative-ion source is a commercial cesium-sputter negative-ion source [21]. Its basic principles of operation are straightforward. Positively charged cesium ions are accelerated toward a cesium-coated aluminum pellet (the ''sputter probe'') at energies of ~2 keV. Particles sputtered from the surface of the aluminum produce low-velocity atoms that become negatively charged as they leave the cesiated surface of the target. Negative ions that are produced from the pellet are accelerated from the target through an exit aperture and are further accelerated as they travel toward the extraction electrode. The sputter probe is maintained at −2 kV, yielding a kinetic energy of 2 keV in a region of ground electrostatic potential. After leaving the extraction region, the Al^- beam was mass selected using a Wien filter.

In separate earlier diagnostic experiments on the ion source, the ion beam was mass analyzed using a magnetic sector mass spectrometer, which has a higher mass resolution than the Wien filter used in this experiment. Two mass peaks were resolved at mass 27 and 28, with the mass-28 peak approximately twice as intense as the mass-27 peak. The intensity ratio of the two mass peaks remained constant over several days of ion source operation. A study using photoelectron spectrometry demonstrates that the mass-28 peak has the same electron affinity as Si^-. The mass-28 peak is thus shown to be Si^-, arising from Si impurities in the aluminum pellet. During the experiments reported here, the Wien filter could not resolve mass 27 and mass 28, because the Wien filter was optimized for high transmission rather than high mass resolution. When the Wien filter was tuned to the high-mass side of the peak, no photodetachment signal was observed for photon energies near the photodetachment threshold of Al^-. A photodetachment signal was observed when the Wien filter was tuned to the low-mass side of the peak. All of the measurements reported here were taken with the Wien filter tuned to the low-mass side of the peak.

The ion beam then entered the interaction region, where it was deflected by 90° with an electrostatic quadrupole deflector [22] before entering an equipotential interaction tube that was floating at a potential of +980 V, as shown in Fig. 2. As a result, the energy of the ion beam was increased to 2980 eV. The pressure in the interaction region was maintained at 2.7×10^{-6} Pa (2×10^{-8} Torr) throughout the experiment. The Al^- beam overlaps a F center laser beam over the entire length of the 50-cm-long stainless steel tube. The long interaction region greatly enhances signal rates as compared to crossed-beam techniques. The entrance and exit apertures on the interaction tube were 1.5 mm in diameter. The laser

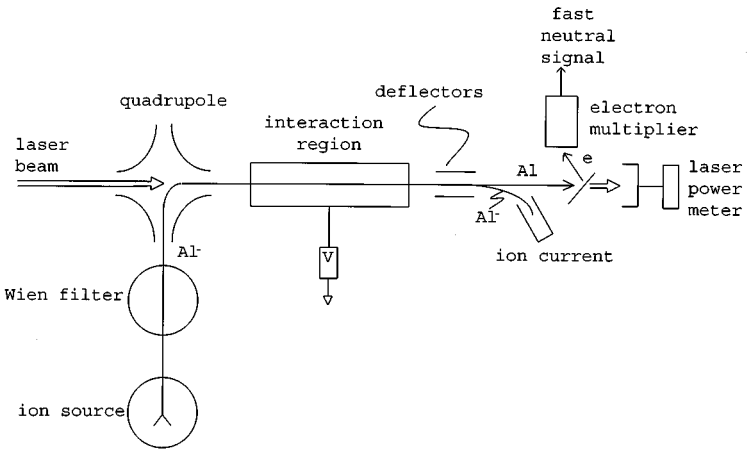

FIG. 2. Schematic diagram of the experimental apparatus. A 2-keV beam of Al^- ions is extracted from a sputter ion source, mass selected by a Wien filter, and deflected by an electrostatic quadrupole into coincidence with an infrared laser beam. The ions accelerate to 2.98 keV in the interaction region, where a fraction of the ions are photodetached by the laser beam, producing fast (≈3 keV) neutral atoms. The ions are then electrostatically deflected into a Faraday cup, while the neutral atoms eject secondary electrons, which are detected by an electron multiplier.

beam was carefully aligned with the ion beam to maximize the overlap between the two interacting beams. The laser and ion beams propagated in the same direction for this experiment.

The fast neutral atoms produced in the interaction region collided with a CaF_2 plate, producing secondary electrons, which were collected by an electron multiplier operating in a linear, charge-amplifying mode. The gain was of the order of 10^6. The output of the electron multiplier was detected by a fast homemade electrometer, with an effective resistance of 100 MΩ (0.1 V/nA) and a bandwidth of at least 3 kHz. The laser beam was mechanically chopped, and the electrometer output was synchronously detected with a lock-in amplifier referenced to the chopper. This discriminated against fast neutral signals resulting from collisional stripping by apertures or by background gas in the interaction tube.

All ions remaining in the beam after interaction with the laser were electrostatically deflected and collected into a Faraday cup. Typical ion currents were 150–250 pA (measured in the Faraday cup), at the maximum of the unresolved mass 27/28 peak. Further details of the coaxial ion-laser beams apparatus are published elsewhere [23].

The laser beam was produced with a Burleigh model FCL-20 laser [24]. An Ar^+ laser pumped KCl:Li crystal was used as the gain medium to give a tunable wavelength range of 2400–2900 nm. In the present experiment, the wavelength scan ranged from 2420 to 2820 nm with a resolution of 0.1 nm (1.6×10^{-5} eV). A suitable pump laser was not available for operating the color-center laser at wavelengths longer than 2820 nm. The wavelength was determined by the grating of the color-center laser, which was calibrated with a Burleigh WA-201R Wavemeter. The frequency of the laser in the rest frame of the ion is less than the frequency measured in the laboratory frame, due to the Doppler effect. At a beam energy of 2980 eV, the fractional redshift is 4.87×10^{-4}. The laser's output power was measured with a Scientech (Model 36-2002) power meter and ranged from 1 to 15 mW over the entire tunable wavelength region. During the measurement, the laser power was monitored after passage through the interaction region with a PbSe detector and fast preamplifier. The output of the PbSe detector was then monitored with a second lock-in amplifier, giving a signal proportional to the laser power.

Because of extracavity and intracavity water absorption lines that occurred over the entire laser scan range, there were many instances where the laser power dropped to a value near zero. As a result, we selected wavelengths at which atmospheric water lines were not a problem. The smallest scan interval was limited to 10 nm, yielding an effective energy step of 1.6×10^{-3} eV. A signal-to-noise ratio of 10:1 was achieved, since this scheme yielded very low background signals. Finally, at each data point the fast neutral signal was normalized to the ion beam current and to the laser power. Although the aluminum and silicon mass peaks are not resolved, it was noted above that the intensity ratio of aluminum to silicon was found to be unchanged over several days of ion source operation, and normalizing to the ion beam current is therefore a valid procedure.

III. RESULTS AND DISCUSSION

The expected signal strength and background rate could only be estimated roughly, because the absolute cross sections for photodetachment and collisional stripping are unknown. When typical values for the cross section for photodetachment (10^{-21} m^2) and collisional stripping (10^{-19} m^2) are inserted using the equations in Marawar *et al.* [25], the estimated photodetachment rates and collisional stripping rates are each a few hundred Hz, in rough agreement with observation.

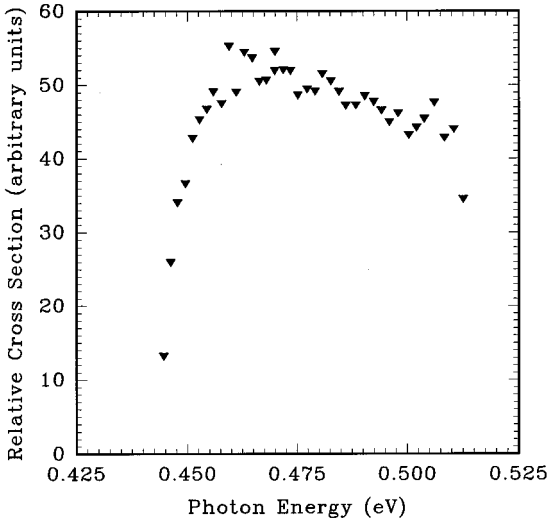

FIG. 3. Relative photodetachment cross section of Al^- as a function of photon energy. All the data points are displayed here.

The results of the present experiment are shown in Fig. 3. Each Doppler-corrected data point was normalized to the ion beam current and to the laser power. At wavelengths above 2820 nm (0.4396 eV), the output power of the *F*-center laser decreased dramatically because the KCl:Li crystal in the FCL laser reached the limit of its gain curve. Uncertainties were estimated for individual data points from the scatter in an individual point at the lock-in detector, giving an estimated relative uncertainty of 10%.

The first stage of the analysis was the extraction of the electron affinity of aluminum, made possible by the steepness of the curve near threshold. To extract the electron affinity of Al, the data were fitted to two theories, the Wigner threshold law [5] and the ZCC theory of photodetachment [19]. In the former case, the Wigner threshold law is valid near threshold only. However, there is little theoretical guide for its range of validity. According to Eq. (1), the shape of the photodetachment curve depends upon the angular momentum of the outgoing electron. As a result of conservation of angular momentum, the detachment of the *p* electron from Al^- yields an outgoing *s* or *d* wave. Since the *d*-wave contribution to the cross section rises very slowly above threshold, the *s*-wave contribution will dominate near threshold.

In the ZCC theory of photodetachment, it is assumed that (1) the initial and final states can be written as a product of wave functions of a neutral core of radius r_0 and a single extra electron; (2) the wave function of the neutral core is unchanged during the process; (3) the neutral core does not contribute to the process; and (4) the potential outside r_0 is negligible. This semiempirical model yields analytical expressions for photodetachment cross sections [19]. Farley [9] has analyzed these expressions and has shown that near

threshold the photodetachment cross section for a p-orbital electron goes as

$$\sigma \rightarrow \left(\frac{16\pi^2}{9}\right)\left(\frac{m\omega}{h\gamma^4}\right)\left[B_1\left(\frac{k}{\gamma}\right)+B_3\left(\frac{k}{\gamma}\right)^3\right], \tag{3}$$

where the variables B_1 and B_3 are defined by

$$B_1 = 2y(y^2+3y+3)^2/(y+2) \tag{4}$$

and

$$B_3 = \left(\frac{2y}{3y+6}\right)^2 (y^2+3y+3)(y^4+5y^3+15y^2+30y+30). \tag{5}$$

where

$$y = \gamma r_0, \tag{6}$$

$$k = [2m(\hbar\omega - E_0)]^{1/2}/\hbar. \tag{7}$$

and

$$\gamma = (2mE_0)^{1/2}/\hbar. \tag{8}$$

In Eqs. (3)–(8), ω is the angular frequency of the photon, and r_0 is the radius of the neutral atom. Equation (3) contains the Wigner threshold law [5] and the leading correction term. The fitting parameter is the threshold energy E_0. The value of r_0, the radius of the highest-energy occupied core orbital, is taken from the Hartree-Fock calculation of Lu *et al.* [26] to be 1.82 Å.

For each theory, the near-threshold data were fitted as a function of the number of data points in the fits, four being the minimum and 12 the maximum. The near-threshold data are shown in Fig. 4. Since the relative uncertainty of each data point was estimated to be 10% each data point was equally weighted. The results of the least-squares fits, including the value of $E_{\rm thr}$, are recorded in Table II. Each fit yielded consistent results of the photodetachment threshold energy.

An average, weighted by the uncertainty in E_0, of all the fits yields an average value of the threshold energy $E_0 = 0.44393 \pm 0.000\,24$ eV. This is only an approximation to the electron affinity of aluminum, because a correction must be applied for unresolved fine structure. The experiment cannot resolve the various fine-structure transitions $^3P_{0,1,2} \rightarrow {}^2P_{1/2,3/2}$. The observed threshold is a weighted average over all possible J''-J' transitions between the negative ion and neutral atom. Each transition will have its own threshold, with an intensity weighted according to the intensity factors given in Table I. We assume that the initial ion populations are given by the statistical weights of the ionic states. This is equivalent to assuming that the population of ions from the ion source corresponds to a temperature that greatly exceeds the fine-structure splittings in the ion. The maximum-energy splitting ($^3P_0 - {}^3P_2$) in the ion is 0.0094 eV, corresponding to a temperature of 114 K. In contrast, the sputter source is believed to operate by ''local vaporization,'' with a temperature of several thousands of degrees. Corderman, Engelking, and Lineberger [27] observed electronic temperatures of 1500±500 K and vibrational temperatures of 5000±1000 K in photoelectron spectrometry studies of O_2^- and FeO^-. Therefore the assumption of statistical populations of the fine-structure states is very reasonable.

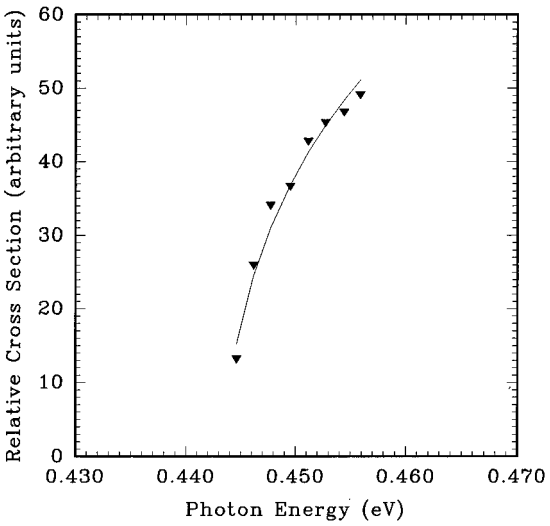

FIG. 4. Relative photodetachment cross section of Al^- as a function of photon energy, showing only the near-threshold region of Fig. 3. The continuous line is a least-squares fit using the Wigner law.

A source of systematic error in determining the electron affinity of Al involved the contribution of the metastable $^1D_2$ state of Al^- to the photodetachment process. The effect of the metastable state on the extracted value of the electron affinity was determined by applying the ZCC model to calculate the photodetachment cross sections resulting from the ground and excited metastable states of Al^-. The results showed that the photodetachment cross section from the excited metastable state of Al^- decreases monotonically at photon energies near the detachment threshold of ground

TABLE II. Sample results of the fitting procedure for both the Wigner threshold law (Ref. [5]) and the ZCC model of photodetachment (Refs. [9,19]). N is number of data points included in the fit. E_0 is the threshold energy returned by the fit. The average value of all fits yields a threshold energy of 0.44393±0.00024 eV, a value that must be corrected for unresolved fine structure in order to obtain the electron affinity.

Fitting equation	N	E_0 Threshold energy
$a(\hbar\omega - E_0)^{1/2}$	4	0.44343±0.00029
$a(\hbar\omega - E_0)^{1/2}$	8	0.44342±0.000937
$a(\hbar\omega - E_0)^{1/2}$	10	0.44301±0.00056
$a(\hbar\omega - E_0)^{1/2} + b(\hbar\omega - E_0)^{5/2}$	4	0.44414±0.00008
$a(\hbar\omega - E_0)^{1/2} + b(\hbar\omega - E_0)^{5/2}$	6	0.44399±0.00017
$a(\hbar\omega - E_0)^{1/2} + b(\hbar\omega - E_0)^{5/2}$	8	0.44394±0.00014
$a(\hbar\omega - E0)^{1/2} + b(\hbar\omega - E_0)^{5/2}$	10	0.44378±0.00029
$a(\hbar\omega - E_0)^{1/2} + b(\hbar\omega - E_0)^{5/2}$	12	0.44372±0.00030
ZCC	4	0.44393±0.00024
ZCC	6	0.44385±0.00019
ZCC	8	0.44367±0.00025
ZCC	10	0.44346±0.00035
ZCC	12	0.44309±0.00051

state Al^-. Data could not be acquired at or below threshold (because of the limited range of the laser), and hence the energy range at which the cross section vanishes could not be experimentally probed. This introduces a systematic error in the data that yields an overall asymmetric error bar in the value of the electron affinity of Al. To estimate this error, the data were fitted again by assuming that the data point closest to threshold corresponded to a vanishing cross section. These fits show that the average value of the threshold energy E_0 can increase by a maximum of 0.000 46 eV due to the presence of an unknown fraction of ions in the metastable $^1D_2$ state in the ion beam. This is one contribution to the overall uncertainty.

The correction due to unresolved fine structure was determined by calculating the weighted average of all the transitions [20]. The weighting factors were shown in Table I. The fine structure for $Al^-(^3P_{0,1,2})$ was obtained by isoelectronic extrapolation by Feigerle, Corderman, and Lineberger [17]. The extrapolated ^3P energy differences for the $0\rightarrow1$ and $0\rightarrow2$ J'' splittings are $0.0032\pm0.000\,37$ eV (26 ± 3 cm^{-1}) and $0.0094\pm0.000\,87$ eV (76 ± 7 cm^{-1}), respectively. The fine structure for neutral $Al(^2P_{1/2,3/2})$ was obtained from Moore's tables [28], and is essentially exact on this energy scale: The ^2P energy difference for the J' splitting is 0.0139 eV (112 ± 0.01 cm^{-1}). The calculation reveals the shift between the experimental threshold (the weighted average of all transitions) and the electron affinity, which is the transition from the lowest-energy sublevel of the ion to the lowest-energy level of the neutral atom, i.e., the $^3P_0\rightarrow{}^2P_{1/2}$ transition energy. The calculation shows that the threshold energy E_0 exceeds the electron affinity by $0.002\,995\pm0.000\,42$ eV. This is intuitively plausible because the fine-structure splitting is larger in the neutral atom. This correction of 0.002 995 eV must therefore be subtracted from the threshold energy E_0 of 0.44393 eV to yield the electron affinity of 0.440 94 eV. The uncertainty in the threshold energy of 0.000 24 eV and the uncertainty in the correction of 0.000 42 eV are added in quadrature. In addition, the possibility of a metastable $^1D_2$ population in the Al^- ion beam introduces a unidirectional correction to the measurement in the range of 0 to 0.000 46 eV. Therefore the total uncertainty in the measurement is estimated to be $+0.000\,66$, $-0.000\,48$ eV. The final result for the electron affinity of aluminum is $0.440\,94(+0.000\,66/-0.00048)$ eV.

The new data shed light on the range of validity of the Wigner law and the utility of the leading correction to the Wigner law. The expectations from theory are shown in Fig. 5, reproduced from Fig. 1(b) of Ref. [9]. Figure 5 shows three curves for photodetachment from a p orbital, which is the case for Al^-. The curve labeled W is the Wigner term alone; the curve labeled WL is the Wigner law with the leading correction, while the curve labeled ZCC is the zero-core-contribution formula. In Ref. [9], the ZCC expression is taken to be exact, while the other two curves (W, WL) are merely near-threshold approximations. Figure 5 is calculated for a hypothetical atom with electron affinity of 1.0 eV. The results can be scaled to other atoms using the scaling parameter for the photon energy, expressed as a dimensionless parameter, namely,

$$z=(\hbar\omega-E_0)/E_0, \tag{9}$$

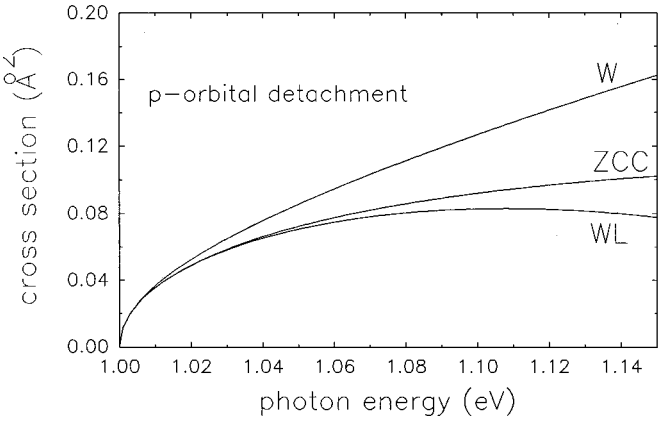

FIG. 5. Comparison of three theoretical predictions of the threshold behavior for photodetachment from a p orbital, using the zero-core-contribution approximation (ZCC), the Wigner law (W), or the Wigner law with the leading correction (WL). The electron affinity is assumed to be exactly 1.0 eV. Scaling to other ions with different electron affinities is possible using Eq. (11).

where E_0 is the electron affinity. Therefore points at a photon energy of (for example) 7% above threshold should correspond.

Comparison of Fig. 3 and Fig. 5 shows that the ZCC approximation differs from the experimental data. In the near-threshold range, both the experimental cross section and the theoretical curves rise sharply with photon energy. Beyond the near-threshold range (up to 3% above threshold), however, there is disagreement: While the ZCC approximation (Fig. 5) continues to rise with photon energy up to a photon energy 15% above threshold, the experimental cross section (Fig. 3) peaks at photon energy of 460–465 meV (approximately 5% above threshold), and then declines by about 14% from the peak as the photon energy increases to 510 meV (a photon energy 15% above threshold). (The data point with the highest photon energy is excluded from this trend because it is discrepant.)

In analyzing the data, one approach is to attempt to perform a least-squares fit to the experimental data using the equation

$$y=(x-x_0)^p, \tag{10}$$

in which both the threshold energy x_0 and the exponent p are varied in order to optimize the fit. However, this procedure is only feasible with very high signal-to-noise ratios. Equation (10) is well known [29] to be very sensitive to even small amounts of noise. In the present work, Eq. (10) is used to investigate the range of validity of the Wigner threshold law. The approach is to use the experimentally determined photodetachment threshold, and the exponent given by the Wigner theory, in order to investigate how well the Wigner theory agrees with the experimental data as the energy of the incident photon increases above threshold.

In Fig. 6, the experimental data are compared with the Wigner threshold law, which for Al^- is proportional to $(E-E_0)^{1/2}$. The Wigner law is fitted to the first 12 experimental data points above threshold. The range of validity of

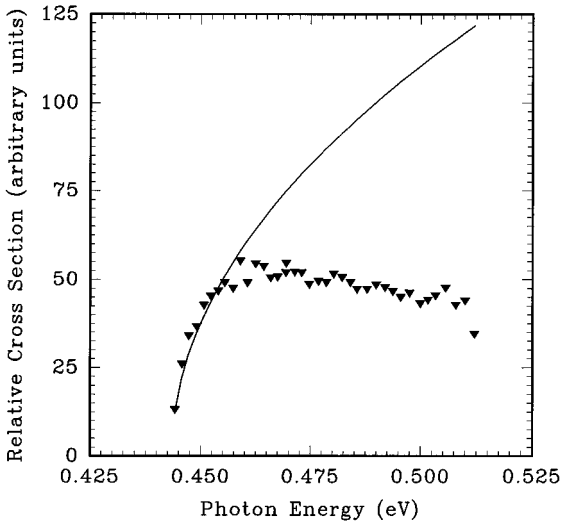

FIG. 6. Experimental data compared with the Wigner threshold law, which for Al^- is proportional to $(E-E_0)^{1/2}$. The Wigner law is fitted to the first 12 experimental data points above threshold. The theory fits the data well in the range 443–456 meV, but poorly elsewhere. The range of validity of the Wigner law at the level of a few percent is approximately 13 meV (3% of the threshold energy) at the level of a few percent.

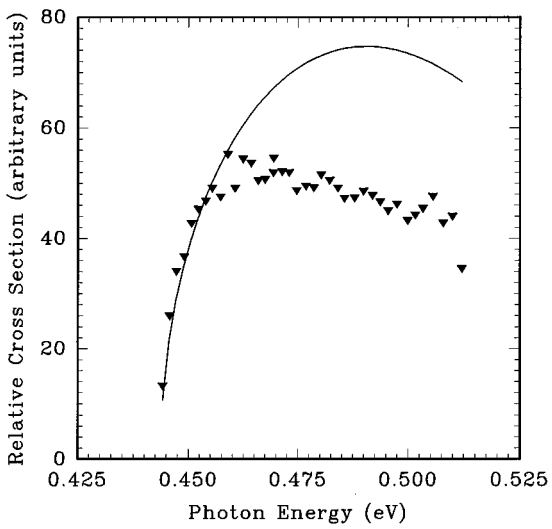

FIG. 7. Experimental data compared with the Wigner law with the leading correction, a term proportional to $(E-E_0)^{3/2}$. The Wigner law (with leading correction) is fitted to the first 12 data points above threshold. In the photon energy range 443–456 meV, the fit is good, but it is poor elsewhere. The range of validity at the level of a few percent is thus 13 meV, or 3% of the threshold energy. Comparison with Fig. 6 shows that the range for which the theory is a good fit is unchanged. However, the addition of the leading correction term does result in improvement in the fit at photon energies above 456 meV. The discrepancy between theory and experiment is still large: the theory is 44% larger than the experimental data at a photon energy of 475 meV, and 60% larger at a photon energy of 510 meV.

the Wigner law (agreement between theory and experiment within a few percent) is approximately 13 meV.

In Fig. 7, the experimental data are compared with the Wigner law with the leading correction, a term proportional to $(E-E_0)^{3/2}$. The Wigner law (with leading correction) is fitted to the first 12 data points above threshold. Comparison with Fig. 6 shows that the amended threshold law is a good fit (theory agrees with experiment within a few percent) for photon energies in the range 443–456 meV, or 3% of the threshold energy. However, addition of the leading correction results in an improvement in the fit outside this range.

Quantitative comparison is shown in Table III, showing the cross sections at photon energies 7% above threshold and 15% above threshold. The theory with the Wigner term alone is 1.65 times the experimental data at a photon energy that is 7% above threshold (475 meV), and is 2.8 times the experimental data at a photon energy that is 15% above threshold (510 meV). In other words, the discrepancy is 65% at a photon energy 7% above threshold, and the discrepancy is 180% at a photon energy 15% above threshold. When the leading correction is included, the discrepancy with experiment shrinks to 44% at 7% above threshold, and to 60% at 15% above threshold. (In this paragraph, the apparent threshold of 443 meV is used; i.e., the corrections for unresolved fine structure are omitted.)

TABLE III. Accuracy of Wigner law, with and without the leading correction. W is the Wigner law alone, WL is the Wigner law with the leading correction, T is theory, and E is experiment.

Photon energy above threshold (%)	$(T\text{-}E)/E$ (%) Theory	
	W	WL
7	65	44
15	180	60

Note that the Wigner law, with leading correction, is still an overestimate of the experimental data, in contrast with the theory (Fig. 5), where the leading correction is predicted to overcorrect, so that WL is predicted to be an underestimate. Certainly, the leading correction is the right order of magnitude to indicate the accuracy of the Wigner law. However, in order to bring the Wigner law into complete agreement with these experimental data, the leading correction would have to be 3 times larger at a photon energy 7% above threshold, and 1.5 times larger at a photon energy 15% above threshold. The inclusion of the leading correction does not make the Wigner law really accurate beyond the near-threshold region (3% above threshold). Instead, the leading correction gives an idea of the accuracy of the Wigner law as one moves away from threshold, giving the discrepancy within a factor of 1.5 to 3.

The theory predicts that the WL approximation (Wigner with leading correction) should track the cross section to within a few percent up to a photon energy of 10–12 % above threshold. Instead, the WL approximation only works up to about 3% above threshold.

In conclusion, the Wigner law is predicted to overestimate the cross section, and it does. Addition of the leading correction to the Wigner law tends to reduce the disagreement with the cross section, as the theory predicts. Finally, the leading correction gives a rough estimate of the accuracy of the Wigner law.

IV. CONCLUSION

The relative photodetachment cross sections of Al^- have been measured near threshold using a merged ion–laser-

beam technique. The near-threshold data were fitted to the Wigner threshold law [5] and the zero-core-contribution model of photodetachment. The photodetachment threshold energy that was returned by the fits is a number of unresolved transition between fine-structure states of the negative ion and neutral atom. A correction must be applied to the observed threshold in order to obtain the electron affinity of aluminum, which is defined as the transition from the lowest-energy state of the ion to the lowest-energy state of the neutral atom ($^3P_0 \rightarrow {}^2P_{1/2}$). The resulting value for the electron affinity of Al is 0.44094 ($+0.000\,66/-0.000\,48$) eV.

The Wigner law is accurate within a few percent of the cross section only for a range of photon energies within 3% above threshold. Above that range, the Wigner law is an overestimate of the experimental cross section, with the theory rising to 2.8 times the cross section at a photon energy 15% above threshold. The addition of the leading correction reduces the discrepancy with experiment, but still does not extend the range of high accuracy (agreement within a few percent) beyond the range of the Wigner law alone. Instead, the leading correction serves to indicate (within a factor of 1.5 to 3) the discrepancy between the Wigner law and the experimental data. The theoretical work of Farley [9] is more of a guide to the reliability of the Wigner law than a full-fledged theory. It is hoped that the present experimental work stimulates renewed theoretical attention to this problem, and the recent work of Liu and Starace [10] is very welcome.

ACKNOWLEDGMENTS

We would like to acknowledge invaluable technical assistance from Heinz Knocke. Financial support from the NSF is gratefully acknowledged for D.C., A.M.C., and J.S.T. under Cooperative Agreement OSR 93-53227, for R.W.M. and J.W.F. under Grant No. PHY 91-22036. Financial support from the DOE is gratefully acknowledged for J.W.F. and R.W.M. under Grant No. DE-FG02-91ER75667.

[1] H. S. W. Massey, *Negative Ions*, 3rd ed. (Cambridge University Press, London, 1976); Smirnov, *Negative Ions* (McGraw-Hill, New York, 1982).
[2] R. Wildt, Astrophys. J. **89**, 295 (1939).
[3] J. Simons and K. D. Jordan, Chem. Rev. **87**, 535 (1987).
[4] Thomas M. Miller, Adv. Electron. Electron. Phys. **55**, 119 (1981).
[5] Eugene P. Wigner, Phys. Rev. **73**, 1002 (1948).
[6] Thomas F. O'Malley, Phys. Rev. **137**, A1668 (1965).
[7] Paul C. Engelking, Phys. Rev. A **26**, 740 (1982).
[8] David R. Herrick and Paul C. Engelking, Phys. Rev. A **29**, 2421 (1984); Paul C. Engelking and David R. Herrick, *ibid.* **29**, 2425 (1984).
[9] John W. Farley, Phys. Rev. A **40**, 6286 (1989).
[10] Chien-Nan Liu and Anthony F. Starace, Bull. Am. Phys. Soc. **41**, 1095 (1996). Liu and Starace found a resonance in the cross section at high enough photon energies to leave the neutral aluminum atom in an excited state. Such a resonance was also found experimentally and reported in B. J. Davies, C. W. Ingram, and D. J. Larson, Bull. Am. Phys. Soc. **41**, 1095 (1996).
[11] W. C. Lineberger and B. W. Woodward, Phys. Rev. Lett. **25**, 424 (1970).
[12] H. Hotop, T. A. Patterson, and W. C. Lineberger, Phys. Rev. A **8**, 762 (1973).
[13] D. Feldmann, Chem. Phys. Lett. **47**, 338 (1977).
[14] H. Hotop and W. C. Lineberger, J. Chem. Phys. **58**, 2379 (1973).
[15] K. R. Lykke, K. K. Murray, and W. C. Lineberger, Phys. Rev. A **43**, 6104 (1991).
[16] H. Hotop and W. C. Lineberger, J. Phys. Chem. Ref. Data **14**, 731 (1985).
[17] C. S. Feigerle, R. R. Corderman, and W. C. Lineberger, J. Chem. Phys. **74**, 1513 (1981).
[18] D. M. Neumark, K. R. Lykke, T. Andersen, and W. C. Lineberger, Phys. Rev. A **32**, 1890 (1985).
[19] R. M. Stehman and S. B. Woo, Phys. Rev. A **20**, 281 (1979).
[20] P. C. Engelking and W. C. Lineberger, Phys. Rev. A **19**, 149 (1979).
[21] Kingston Scientific Inc., Kingston, TN 37763.
[22] John W. Farley, Rev. Sci. Instrum. **56**, 1834 (1985).
[23] Mohammad Al-Za'al, Harold C. Miller, and John W. Farley, Phys. Rev. A **35**, 1099 (1987); John W. Farley, in *Laser Techniques for State-Selected and State-to-State Chemistry*, edited by C.-Y. Ng, Proc. SPIE No. 1858 (SPIE, Bellingham, WA, 1993), p. 92.
[24] Burleigh Instruments Inc., Fishers, NY 14453.
[25] R. W. Marawar, Daniel C. Cowles, Raymond E. Keeler, Andrew P. White, and John W. Farley, Rev. Sci. Instrum. **65**, 2769 (1994).
[26] C. C. Lu, T. A. Carlson, F. B. Malik, T. C. Tucker, and C. W. Nestor Jr., At. Data **3**, 1 (1971).
[27] Reed R. Corderman, P. C. Engelking, and W. C. Lineberger, Appl. Phys. Lett. **36**, 533 (1980).
[28] C. E. Moore, Natl. Bur. Standards (U.S.), Circ. No. 467 (1949).
[29] J. B. Donohue, P. A. M. Gram, M. V. Hynes, R. W. Hamm, C. A. Frost, H. C. Bryant, K. B. Butterfield, D. A. Clark, and W. W. Smith, Phys. Rev. Lett. **48**, 1538 (1982).